Electronic Supplementary Information

Improving the photoelectrocatalytic efficiency of $CuWO_4$ through molybdenum for tungsten substitution and coupling with $BiVO_4$

Annalisa Polo,[a] Maria Vittoria Dozzi,*[a] Gianluigi Marra,[b] Kevin Sivula[c] and Elena Selli[a]

[a]*Dipartimento di Chimica, Università degli Studi di Milano, Via Golgi 19, 20133 Milano, Italy. E-mail: mariavittoria.dozzi@unimi.it*

[b]*Eni S.p.A Novara Laboratories (NOLAB), Renewable, New Energies and Material Science Research Center (DE-R&D), via G. Fauser 4, I-28100 Novara, Italy*

[c]*Laboratory for Molecular Engineering of Optoelectronic Nanomaterials, École Polytechnique Fédérale de Lausanne (EPFL), 1015 Lausanne, Switzerland*

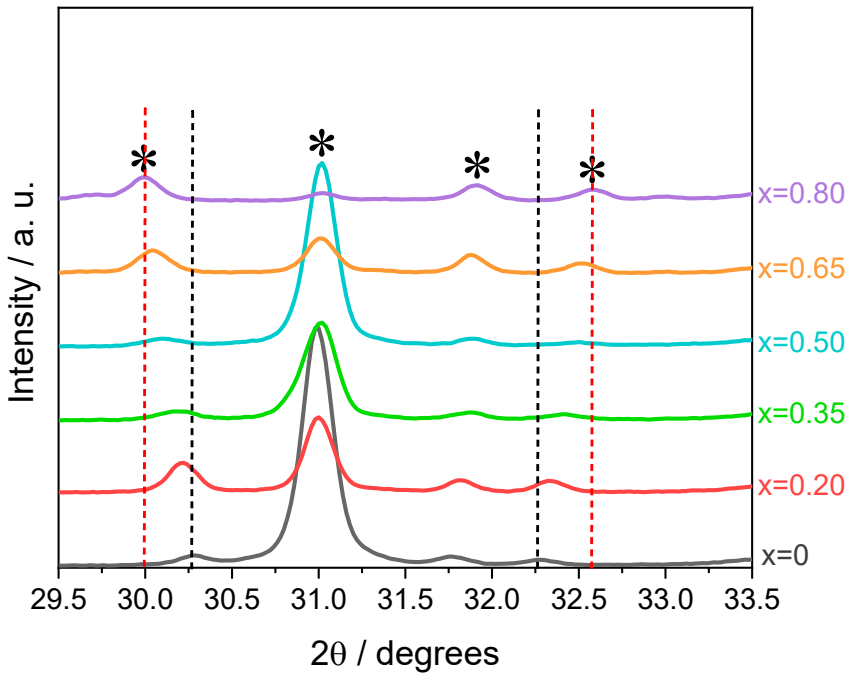

Fig. S1 Detailed view, in the 29.5° – 33.5° 2θ range, of the XRD patterns of $CuW_{1-x}Mo_xO_4$ electrodes ($x = 0 – 0.8$). The asterisks mark the wolframite structure peaks. Wolframite peaks undergo a progressive shift with increasing x value, starting from pure $CuWO_4$ (black dashed lines) to $CuW_{1-x}Mo_xO_4$ with x = 0.8 (red dashed lines).

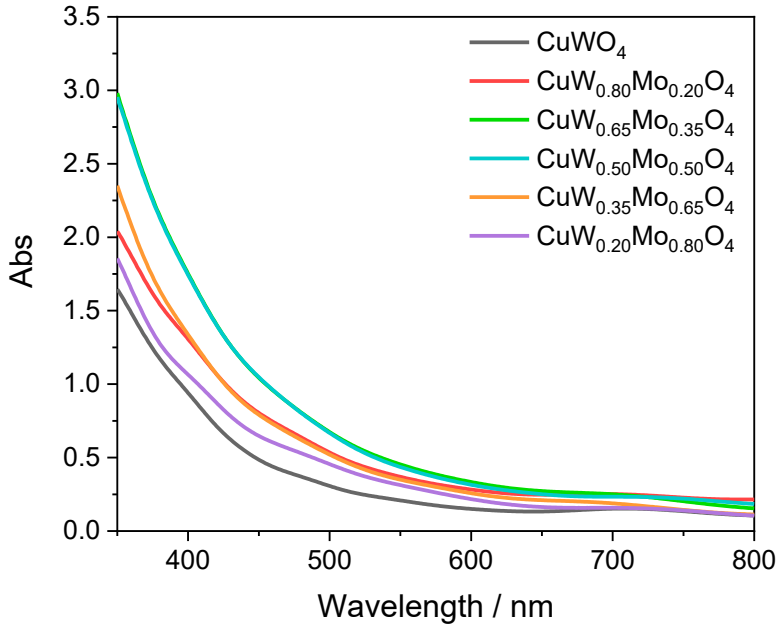

Fig. S2 Absorption spectra of the $CuW_{1-x}Mo_xO_4$ films with different Mo^{6+} for W^{6+} percent substitution.

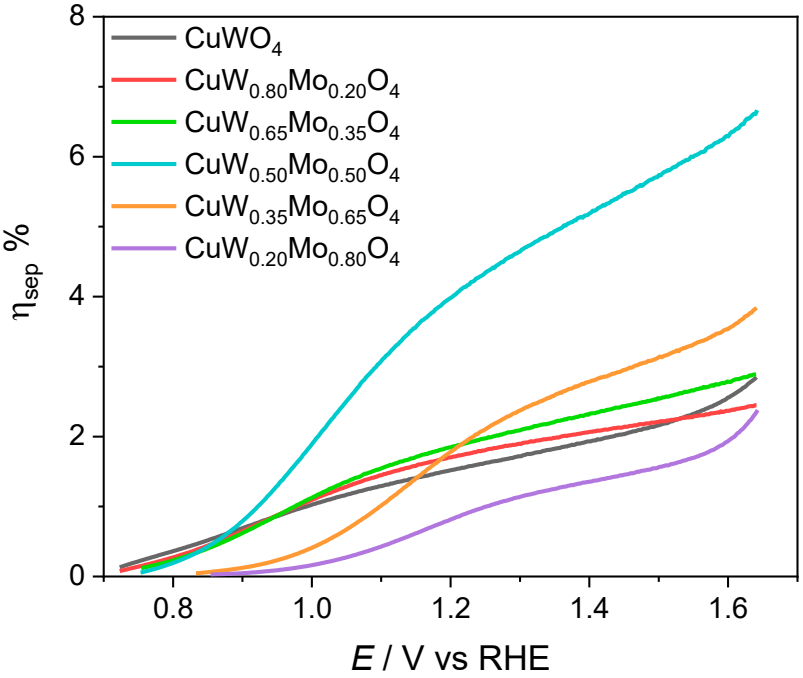

Fig. S3 η_{sep} of $CuW_{1-x}Mo_xO_4$ films with different Mo^{6+} for W^{6+} substitution degrees, under back-side irradiation (see Section S2 below).

S1 Absorption coefficient (α) and absorption depth (δ) calculation

From the absorbance at 420 nm and the thickness of multilayer $CuW_{0.5}Mo_{0.5}O_4$ electrodes, the absorption coefficient (α) of the material at this wavelength was calculated from the Lambert Beer law according to Eq. S1:

$$\alpha = \frac{1}{h} 2.303\, A \tag{S1}$$

where h is the thickness of the film and A is the absorbance at the specific wavelength. We obtained α = 7 x 10^3 nm^{-1} at 420 nm.[1] The absorption depth (δ) of the investigated materials, *i.e.*, the $CuW_{0.5}Mo_{0.5}O_4$ film thickness ensuring 96%, 83% or 63% absorption of 420 nm incident light, calculated as $\delta = 3\ \alpha^{-1}$, $\delta = 2\ \alpha^{-1}$ and $\delta = \alpha^{-1}$, respectively,[2] are reported in Table S1.

Table S1 Calculated penetration depths δ of the $CuW_{0.5}Mo_{0.5}O_4$ 1L material ensuring 96%, 83% or 63% absorption of the incident light at 420 nm.

Percentage of 420 nm light absorbed	δ / nm
63% (1 x α^{-1})	144
83% (2 x α^{-1})	289
96% (3 x α^{-1})	433

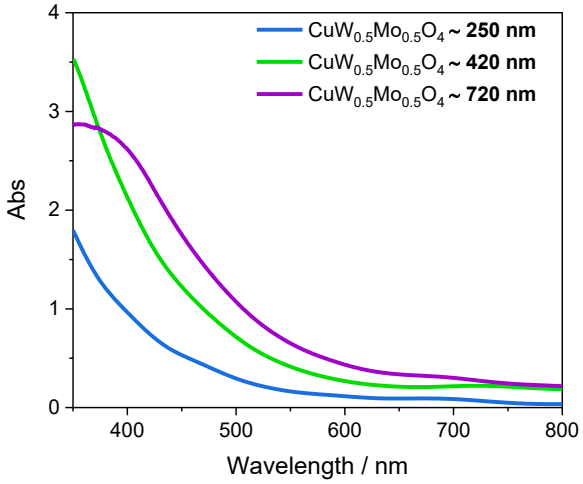

Fig. S4 Absorption spectra of $CuWMo_{0.5}O_4$ 1L, $CuW_{0.5}Mo_{0.5}O_4$ 2L and $CuW_{0.5}Mo_{0.5}O_4$ 3L.

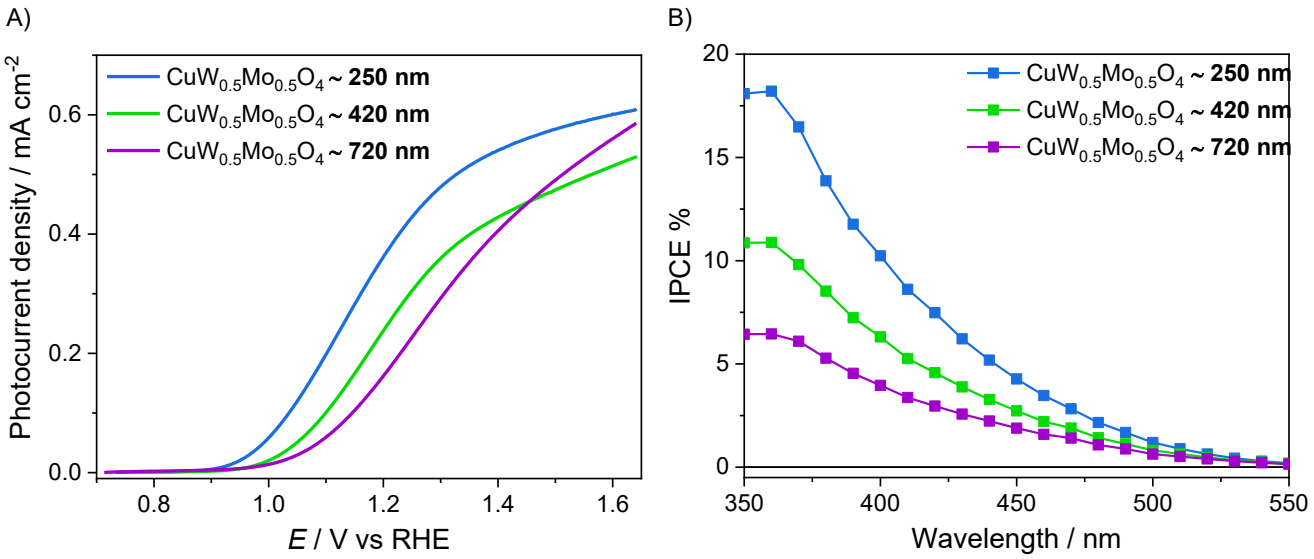

Fig. S5 (A) Linear sweep voltammetry (LSV) scans and (B) incident photon to current efficiency (IPCE) plots recorded at 1.23 V_{RHE} with differently thick $CuW_{0.5}Mo_{0.5}O_4$ electrodes (blue 1L, green 2L and violet 3L) under back-side irradiation.

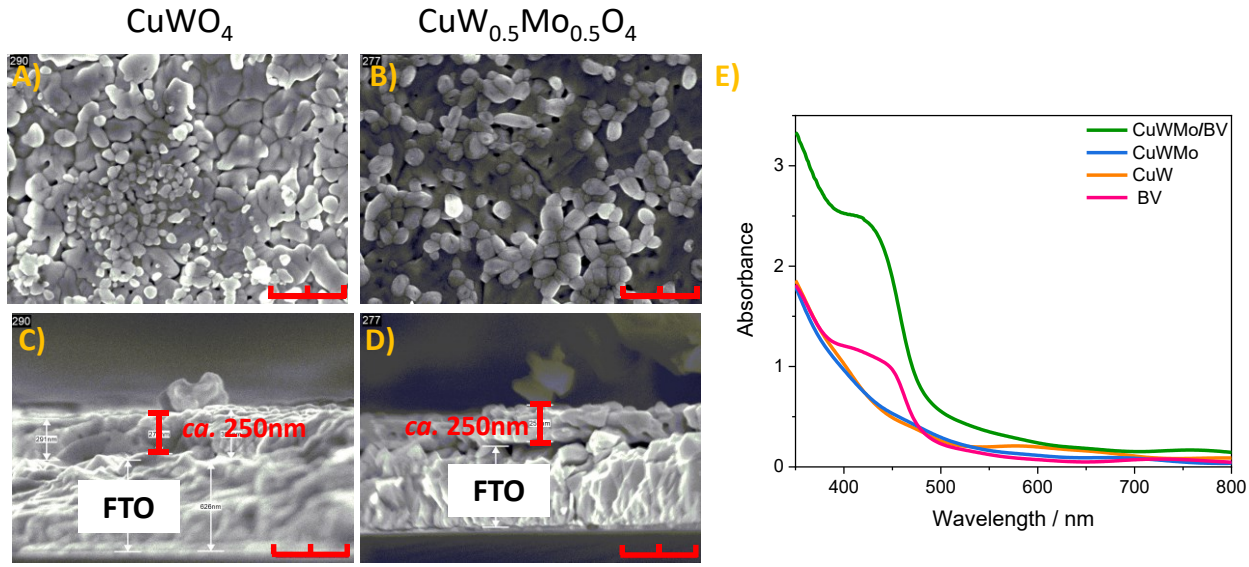

Fig. S6 (A,B) Top view and (C,D) side view SEM images at 50kx magnification of (A,C) CuW and (B,D) CuWMo, with a 500 nm scale bar. (E) Absorption spectra of CuW (orange), CuWMo (blue), BV (magenta) and CuWMo/BV (green).

S2 η_{sep} and η_{inj} calculation from LSV measurements in the presence of $NaNO_2$ as hole scavenger

We evaluated the charge separation efficiency in the bulk (η_{sep}), that is the fraction of photogenerated holes that successfully reach the electrode/electrolyte interface without recombining with electrons in the bulk, and the charge injection efficiency at the film/electrolyte interface (η_{inj}), *i.e.*, the fraction of photogenerated holes that, upon reaching the electrode/electrolyte interface, are successfully injected into the electrolyte. $NaNO_2$ was employed as hole scavenger for copper tungstate materials,[3] and LSV measurements performed in contact with either a K_3BO_3 buffered solution ($J_{K_3BO_3}$), or the buffered solution also containing $NaNO_2$ (J_{NaNO_2}), under the assumption that no charge accumulation occurs at the semiconductor-liquid junction.[4] The injection efficiency was determined as $\eta_{\mathrm{inj}} = J_{\mathrm{K_3BO_3}}/J_{\mathrm{NaNO_2}}$ and the separation efficiency was calculated as $\eta_{\mathrm{sep}} = J_{\mathrm{NaNO_2}}/J_{\mathrm{abs}}$, J_{abs} being the theoretical maximum photocurrent density of the material, corresponding to 100% conversion of the absorbed photons into photocurrent, which can be calculated from the integration of the absorption spectrum of the photoactive material over the AM 1.5 G solar spectrum. The calculated η_{inj} and η_{sep} are usually plotted as a function of the applied potential.

S3 Intensity modulated photocurrent spectroscopy (IMPS) measurements

The IMPS response in Fig. S6 was fit to a proper phenomenological model,[5,6] according to the following equation:[7]

$$J(\omega) = \frac{J_h}{1 + (i\omega\tau_h)^{\alpha_1}} - \frac{J_r}{1 + (i\omega\tau_r)^{\alpha_2}} \quad \text{(S2)}$$

From the fit model, the following parameters can be calculated: J_h, the flux of holes arriving to the SCLJ and available for water oxidation; J_r, the flux of holes that are lost due to recombination at the film surface; and the two time constants τ_h, for bulk hole current, and τ_r, for surface recombination. α_1 and α_2

are the non-ideality factors used to describe the deformation of the semicircles due to the frequency dependence of the dielectric constant.

In this way, an accurate evaluation of the η_{sep} and η_{inj} parameters *in operando* can be obtained as $\eta_{sep} = J_h/J_{abs}$ (where J_{abs} is the maximum photocurrent expected for each examined photoanode based on its absorption spectrum) and $\eta_{inj} = (J_h - J_r)/J_h$.

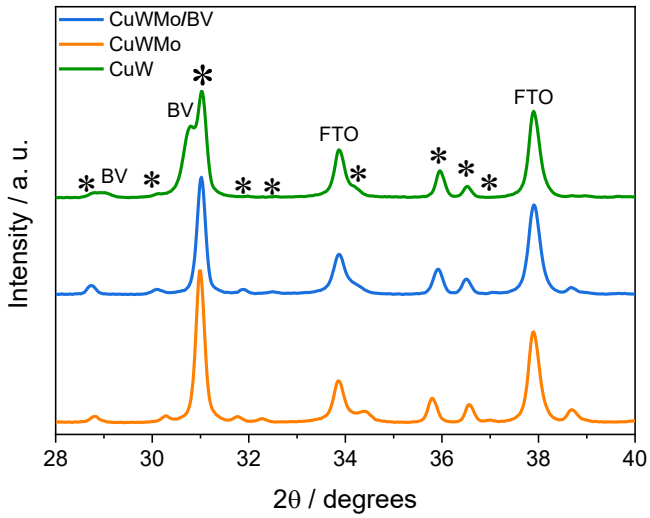

Fig. S7 **(**A) XRD patterns in the 28° to 40° 2θ region of CuW, CuWMo and CuWMo/BV films. The $CuW_{0.5}Mo_{0.5}O_4$ wolframite reflections are marked with an asterisk. FTO and $BiVO_4$ (BV) reflections are also indicated.

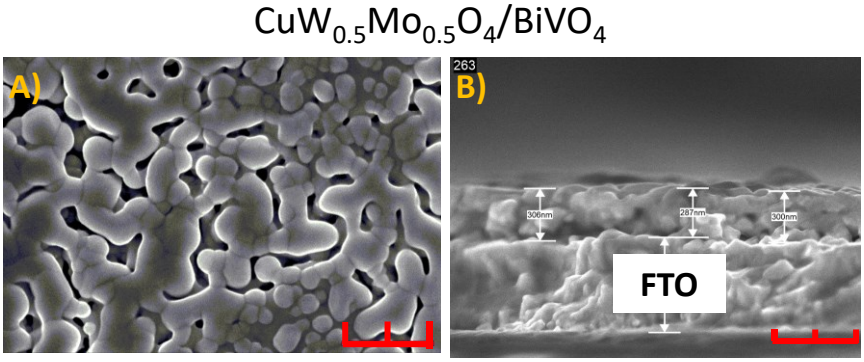

Fig. S8 **(**A) Top and (B) side view SEM images at 50kx magnification of CuWMo/BV heterojunction electrode. The scale bar is 500 nm.

References

1 W. Q. Hong, *J. Phys. D. Appl. Phys.*, 1989, **22**, 1384–1385.

2 S. Murcia-López, C. Fàbrega, D. Monllor-Satoca, M. D. Hernández-Alonso, G. Penelas-Pérez, A. Morata, J. R. Morante and T. Andreu, *ACS Appl. Mater. Interfaces*, 2016, **8**, 4076–4085.

3 A. Polo, C. Nomellini, I. Grigioni, M. V. Dozzi and E. Selli, *ACS Appl. Energy Mater.*, 2020, **3**, 6956–6964.

4 H. Dotan, K. Sivula, M. Grätzel, A. Rothschild and S. C. Warren, *Energy Environ. Sci.*, 2011, **4**, 958–964.

5 D. Klotz, D. S. Ellis, H. Dotan and A. Rothschild, *Phys. Chem. Chem. Phys.*, 2016, **18**, 23438–23457.

6 D. Klotz, D. A. Grave and A. Rothschild, *Phys. Chem. Chem. Phys.*, 2017, **19**, 20383–20392.

7 F. Boudoire, Y. Liu, F. Le Formal, N. Guijarro, C. R. Lhermitte and K. Sivula, *J. Phys. Chem. C*, 2021, **125**, 10883–10890.